Journal of Experimental Botany, Vol. 76, No. 22 pp. 6700–6713, 2025
https://doi.org/10.1093/jxb/eraf380 Advance Access Publication 29 August 2025

TECHNICAL INNOVATION

Development of an efficient CRISPR-mediated genome editing platform in the diploid-polyploid model system *Tragopogon* (Asteraceae)

Shengchen Shan[1,*], Michael T. Pisias[2], Zhengzhi Zhang[2], Evgeny V. Mavrodiev[1], Matthew A. Gitzendanner[3], Bernard A. Hauser[3], Corrinne E. Grover[4], W. Brad Barbazuk[3,5], Pamela S. Soltis[1,5,6], Bing Yang[2,7], and Douglas E. Soltis[1,3,5,6]

[1] Florida Museum of Natural History, University of Florida, Gainesville, FL 32611, USA
[2] Division of Plant Science and Technology, University of Missouri, Columbia, MO 65211, USA
[3] Department of Biology, University of Florida, Gainesville, FL 32611, USA
[4] Department of Ecology, Evolution and Organismal Biology, Iowa State University, Ames, IA 50011, USA
[5] Genetics Institute, University of Florida, Gainesville, FL 32610, USA
[6] Biodiversity Institute, University of Florida, Gainesville, FL 32611, USA
[7] Donald Danforth Plant Science Center, St Louis, MO 63132, USA

* Correspondence: shan158538@ufl.edu

Received 3 January 2025; Accepted 25 August 2025

Editor: Scott Boden, The University of Adelaide, Australia

Abstract

Polyploidy or whole-genome duplication (WGD) is a significant evolutionary force. However, the mechanisms governing polyploid genome evolution remain unclear, limited largely by a lack of functional analysis tools in organisms that best exemplify the earliest stages of WGD. *Tragopogon* (Asteraceae) includes an evolutionary model system for studying the immediate consequences of polyploidy. In this study, we significantly improved the transformation system and obtained genome-edited *T. porrifolius* (2*x*) and *T. mirus* (4*x*) primary generation (T_0) individuals. Using CRISPR/Cas9, we knocked out the *dihydroflavonol 4-reductase* (*DFR*) gene, which controls anthocyanin synthesis, in both species. All transgenic allotetraploid *T. mirus* individuals had at least one mutant *DFR* allele, and 71.4% had all four *DFR* alleles edited. The resulting mutants lacked anthocyanin, and these mutations were inherited in the T_1 generation. This study demonstrates a highly efficient CRISPR platform, producing genome-edited *Tragopogon* individuals that have completed the life cycle. The approaches used and challenges faced in building the CRISPR system in *Tragopogon* provide a framework for building similar systems in other non-genetic models. Genome editing in *Tragopogon* paves the way for novel functional biology studies of polyploid genome evolution and the consequences of WGD on complex traits, holding enormous potential for both basic and applied research.

Keywords: CRISPR, genome evolution, non-genetic model, polyploidy, *Tragopogon*, transformation.

Abbreviations: BAP, 6-benzylaminopurine; MS, Murashige & Skoog modified basal medium with Gamborg vitamins; NAA, α-naphthaleneacetic acid; WGD, whole-genome duplication; WPM, Lloyd & McCown woody plant basal medium with vitamins.

Introduction

Polyploidy, also known as whole-genome duplication (WGD), is a major evolutionary force in plants (Soltis *et al.*, 2015; Van de Peer *et al.*, 2021). WGDs generate genetic, phenotypic, and metabolic diversity and are associated with increased evolvability and diversification (Wendel, 2015; Soltis and Soltis, 2016; Landis *et al.*, 2018; Doyle and Coate, 2019; Fox *et al.*, 2020; Van de Peer *et al.*, 2021). All living angiosperms are of ancient polyploid ancestry (Jiao *et al.*, 2011), and 35% of extant vascular plant species may have originated via polyploidy (Wood *et al.*, 2009). In addition, most crops are polyploids (Renny-Byfield and Wendel, 2014), and polyploidy plays an important role in plant breeding (Udall and Wendel, 2006; Sattler *et al.*, 2016). Therefore, a better understanding of polyploid genome function and evolution is essential for both comprehending plant diversity and facilitating crop improvement (Renny-Byfield and Wendel, 2014).

In newly formed allopolyploids (those that arose through hybridization and genome doubling), there are duplicate gene copies (homeologs) with redundant or overlapping expression and function. Over time, these duplicates experience various fates, ranging from retention of both copies with original function to homeolog divergence to loss of one copy via fractionation (Papp *et al.*, 2003; Freeling *et al.*, 2012; Tang *et al.*, 2012; De Smet *et al.*, 2013; Wendel *et al.*, 2018). Some genes are consistently conserved as singletons, implying their single-copy status is advantageous and favored by selection (Paterson *et al.*, 2006; De Smet *et al.*, 2013; Li *et al.*, 2016). In addition, following WGD, genes from one parent may be more highly retained than those of the other (i.e., genomic dominance) (Chaudhary *et al.*, 2009; Evangelisti and Conant, 2010; Wendel *et al.*, 2012). For many other genes, duplicate copies are preserved following WGD, a phenomenon that may be explained by the dosage balance hypothesis (Birchler and Veitia, 2007, 2012), which argues that genes encoding subunits of protein complexes tend to be retained following polyploidy; loss of one copy of these genes may be selected against because of the disrupted stoichiometry of members of multi-subunit protein complexes (Birchler and Veitia, 2007, 2012; Freeling, 2009). Additionally, genes encoding transcription factors are more likely to be retained in duplicate following WGD because loss of one copy of transcription factor genes may have a pleiotropic effect, which would not be observed when losing one copy of genes acting at the termini of genetic networks (Blanc and Wolfe, 2004; Shi *et al.*, 2010). However, despite these various observed gene retention patterns, the mechanisms underlying these patterns remain elusive, primarily due to the lack of functional studies in organisms, especially those from natural systems, that best exemplify the earliest phases of WGD. A better understanding of gene fate following WGD will contribute to an enhanced comprehension of the genetic basis of the success of polyploids.

The diploid–polyploid system in North American *Tragopogon* (Asteraceae) represents a rare evolutionary model for studying the immediate consequences of polyploidy (Ownbey, 1950; Soltis *et al.*, 2004, 2012). The naturally occurring allotetraploids *Tragopogon miscellus* and *T. mirus* formed in the last 95–100 years. The diploid parents of *T. miscellus* are *T. dubius* and *T. pratensis*, and those of *T. mirus* are *T. dubius* and *T. porrifolius*. The two *Tragopogon* polyploids have each formed repeatedly (>10 times) in nature, providing multiple replicates for the study of WGD (Symonds *et al.*, 2010; Soltis *et al.*, 2012). Previous studies have demonstrated that novel arrays of karyotypes, gene content and expression, and epigenetic regulation were generated in these newly formed *Tragopogon* polyploids. Aneuploidy and intergenomic translocations have been found in both natural and synthetic *T. miscellus* and *T. mirus* (Lim *et al.*, 2008; Chester *et al.*, 2012, 2015; Spoelhof *et al.*, 2017). Dynamic genetic changes subsequent to WGD, such as gene loss and gene silencing, have been well documented in both *T. miscellus* and *T. mirus* (e.g. Tate *et al.*, 2009; Buggs *et al.*, 2011, 2012; Boatwright *et al.*, 2018; Shan *et al.*, 2020a; Yoo *et al.*, 2024). In addition, Shan *et al.* (2024a) showed that novel DNA methylation variants can be generated rapidly after polyploidy in *T. miscellus*. Given the extensive spectrum of genetic and epigenetic alterations detected in *Tragopogon* polyploids through cytological and bioinformatic analyses, our subsequent objective is to explore the resulting phenotypic effects of these dynamic genomic changes using functional biology approaches. Achieving this goal necessitates the development of an efficient genome editing system.

The CRISPR/Cas9 system is a powerful genome editing tool (Lander, 2016; Shan *et al.*, 2020b), and we had initial success modifying *Tragopogon* genomes using CRISPR (Shan *et al.*, 2018). However, there are some limitations of the previously described genome-editing platform in *Tragopogon*: (i) hyperhydricity (a physiological disorder that occurs in plant tissue culture) was commonly found in regenerated shoots (Fig. 4 in Shan *et al.*, 2018); (ii) a rooting system was not available, limiting the selection and maintenance of heritable edits beyond the T_0 generation; and (iii) the null *pds* mutant shoots regenerated in Shan *et al.* (2018) lacked roots and photosynthetic pigments and, therefore, could not survive in soil. Improving the regeneration system and obtaining *Tragopogon* individuals that have completed a life cycle and heritable edits will facilitate many novel functional studies in this evolutionary model.

In the current study, we embraced these challenges by improving shoot regeneration, developing an efficient rooting system, and knocking out another target gene, i.e. *DFR* (encoding dihydroflavonol 4-reductase) to further validate the efficacy of our CRISPR/Cas9 system in diploid and tetraploid *Tragopogon*. The *DFR* gene is involved in the flavonoid biosynthetic pathway, which produces anthocyanin (Tanaka *et al.*,

2008). Reduction of dihydroflavonols by DFR leads to corresponding 3,4-*cis*-leucoanthocyanidins, which are immediate precursors of anthocyanidins (Tanaka *et al.*, 2008). The *dfr* mutants are viable in soil conditions, and the T_1 generations have been obtained in model plant species, including rice (*Oryza sativa*) (Jung *et al.*, 2019) and Japanese morning glory (*Ipomoea nil*) (Watanabe *et al.*, 2017). In *Gerbera hybrida* (also from Asteraceae, like *Tragopogon*), the *DFR* expression profile correlated with anthocyanin pigmentation in the inflorescence (Helariutta *et al.*, 1995). Therefore, *dfr* mutants of the diploid *T. porrifolius* and the polyploid *T. mirus* should lack anthocyanin pigmentation, leading to loss of both purple inflorescences and red markings in the leaves. These striking changes in color will facilitate visual identification of mutants and convenient evaluation of the genome editing outcome. In summary, an improved and efficient genome-editing platform in the evolutionary model *Tragopogon* will enable us to gain unprecedented insight into the underlying genetic mechanisms of the early stages of polyploid genome evolution. In addition, this platform will also facilitate plant breeding in Asteraceae, the largest plant family, which contains numerous crops and ornamentals.

Materials and methods

Tragopogon material and seed germination

The diploid *T. porrifolius* line used in this study is from Baker Creek heirloom seed company (voucher Soltis and Soltis 3078). The tetraploid *T. mirus* individual used in the current study was grown from seed collected from a natural population (Soltis and Soltis 3091-3; Pullman, WA, USA). We followed the seed sterilization and germination protocols from Shan *et al.* (2018) with modifications. Briefly, pericarps of *Tragopogon* achenes were carefully removed; the seeds were surface sterilized in 20% bleach with one drop of Tween-20 (working as surfactant) for 20 min and rinsed four times with autoclaved deionized water to remove any residual bleach. The sterilized *Tragopogon* seeds were then placed on the seed germination medium (Supplementary Table S1).

Testing various shooting and rooting media in *T. porrifolius*

To improve the shoot regeneration system and reduce the occurrence of hyperhydricity in *Tragopogon*, we tested the direct shooting efficiency using *T. porrifolius* leaf explants from 2- to 9-week-old seedlings on 11 different shooting media (Table 1). For each medium, at least 88 explants (median: 116) were used, with at least two replicates (mostly three) conducted (Table 1). The shooting results were examined 4–6 weeks after placing the explants on the medium. The shooting rates were calculated by dividing the number of regenerated shoots by the total number of explants.

All tested media were adapted from studies in species that are phylogenetically closely related to *Tragopogon*, including *Chrysanthemum*, *Lactuca*, and *Echinacea* (Table 1). Each medium contained a unique combination of hormones: α-naphthaleneacetic acid (NAA) was used as the source of auxin, and different types of cytokinin, including 6-benzylaminopurine (BAP), thidiazuron (TDZ), and *trans*-zeatin (ZEA), were tested. Coconut water (ZICO Rising, Seal Beach, CA, USA; natural flavor) and activated charcoal were added to certain media (Table 1). We tested two types of gelling agents: gelrite and agargellan. Both Murashige & Skoog modified basal medium with Gamborg vitamins (MS salt) and Lloyd & McCown woody plant basal medium with vitamins (WPM salt) were used to supply macro- and micronutrients as well as vitamins to the explants. In addition, for two experiments (i.e. 'C3 pulse' and 'COCO-1 pulse'), the shooting process comprised two continuous phases: the shoot initiation phase on medium with hormones, and then the shoot elongation phase on MS medium without hormones (4.44 g l^{-1} MS, 30 g l^{-1} sucrose, 5 g l^{-1} gelrite, pH 5.8); this process is also referred to as 'pulse hormone treatment' (Table 1). In contrast, for the rest of the experiments, the explants were placed on the hormone-containing medium during the entire shooting process. Unless otherwise noted, all reagents mentioned above were from PhytoTech Labs (Lenexa, KS, USA).

To develop an efficient root regeneration system, regenerated shoots were placed on four different rooting media (Table 2). The shoots were regenerated from *T. porrifolius* leaf explants. For each rooting medium, at least 39 shoots (median 42) were used for the rooting experiment, with at least four replicates conducted (Table 2). We examined the rooting results after approximately 3 weeks of treatment, and the rooting rates were calculated by dividing the number of rooted shoots by the total number of shoots.

Each rooting medium comprised a distinct combination of hormones. Two types of auxins were tested: NAA and indole-3-butyric acid (IBA); BAP was also added to C3 and WPM-C3 media (Table 2). Either the MS or the WPM salt was added to the rooting medium. In addition, all media employed the pulse hormone treatment approach: after approximately 1 week of treatment on the rooting medium (containing hormones), shoots were transferred to a hormone-free medium for approximately 2 weeks. After treatment with the C3 medium, shoots were moved to the MS medium; shoots were transferred to the WPM medium following the treatment with the WPM-C3, COCO-R, or COCO-R2 medium (Table 2).

Agrobacterium-mediated transformation and plant regeneration

Based on the results from the shooting and rooting experiments described above and our methods from previous studies (Shan *et al.*, 2018, 2023), we have updated the *Tragopogon* transformation and regeneration protocols as outlined below. After placing the *Tragopogon* seeds on the seed germination medium for approximately 2 weeks, the cotyledon explants were harvested and cut into 1 cm segments. To promote *Agrobacterium*-mediated transformation efficiency, the surfaces of the cotyledon segments were slightly scored to create wounds using a sterile blade. The *Tragopogon* cotyledon explants were placed on the callus induction medium (Supplementary Table S1) for 2 d (in the dark at room temperature, at 23 °C) before transformation (a process referred to as 'pre-culture'). After co-cultivation of the explants and *Agrobacterium* (OD_{600}=0.1–0.2) for 30 min, the explants were cultivated on the co-cultivation medium (Supplementary Table S1) for 3 d in the dark at room temperature. The explants were then transferred to the selective callus induction medium (Supplementary Table S1). After 24 d, to initiate the shooting process, calli of *T. porrifolius* and *T. mirus* were transferred to the selective COCO-1 and COCO-3 shooting media, respectively (Supplementary Table S1). The shooting medium was renewed every 2–3 weeks. After 33 d, the calli with tiny shoots were transferred to selective WPM-3 medium (Supplementary Table S1) for shoot elongation. After 15 d, the elongated shoots were gradually transferred (up to 31 d on selective WPM-3 medium) to selective COCO-R medium (Supplementary Table S1) for rooting. The selection and plant regeneration processes were conducted inside a tissue culture incubator [14 h light (52.5 μmol m^{-2} s^{-1})/10 h dark, 25 °C; model CU36L4C8 from Percival Scientific, Perry, IA, USA]. After 45 d, rooted shoots were gradually transferred to soil and continued their growth inside a growth chamber [14 h light (52.5 μmol m^{-2} s^{-1})/10 h dark, 25 °C; model AR-1110 from Percival Scientific]. After approximately 3 months of growth in soil, the regenerated plants were subjected to 3 months of cold treatment [8 h light (52.5 μmol m^{-2} s^{-1})/16 h dark, 7 °C]. The plants were then

Table 1. Shooting media examined in *Tragopogon*

Medium[a]	Shooting rate (%)[b]	Hormones (mg l^{-1})	Other ingredients (g l^{-1})	Explants[c] (replicates)	Reference; genus studied
C3 pulse[d]	0	NAA (2.14), BAP (0.23)	MS (4.44), gelrite (5)	227 (3)	Trigiano *et al*., 2011; *Chrysanthemum*
IA-5	0	NAA (0.1), TDZ (2)	MS (4.44), agargellan (7)	118 (3)	Armas *et al*., 2017; *Lactuca*
IA-6	4.3	NAA (0.1), ZEA (2)	MS (4.44), agargellan (7)	116 (3)	Armas *et al*., 2017; *Lactuca*
IA-7	9.0	NAA (0.05), BAP (1)	MS (4.44), agargellan (7)	189 (3)	Armas *et al*., 2017; *Lactuca*
IA-17	0	NAA (0.125), BAP (2.5)	MS (4.44), agargellan (7), activated charcoal (0.2)	116 (2)	Armas *et al*., 2017; *Lactuca*
IA-18	0	NAA (0.25), BAP (5)	MS (4.44), agargellan (7), activated charcoal (0.2)	101 (2)	Armas *et al*., 2017; *Lactuca*
IA-19	0	NAA (0.5), BAP (10)	MS (4.44), agargellan (7), activated charcoal (0.2)	171 (4)	Armas *et al*., 2017; *Lactuca*
SIM	9.6	NAA (0.1), BAP (0.1)	MS (4.44), agargellan (8)	104 (3)	Hunter and Burritt, 2004; *Lactuca*
COCO	1.1	BAP (2.5)	MS (4.44), agargellan (8.5), 5% (v/v) coconut water	179 (3)	Mechanda *et al*., 2003; *Echinacea*
COCO-1	8.6	BAP (2.5)	WPM (2.41), agargellan (8.5), 5% (v/v) coconut water	93 (3)	Mechanda *et al*., 2003; *Echinacea*
COCO-1 pulse[d]	40.9	BAP (2.5)	WPM (2.41), agargellan (8.5), 5% (v/v) coconut water	88 (3)	Mechanda *et al*., 2003; *Echinacea*

[a]All media contain 30 g l^{-1} sucrose (which is not listed in the 'Other ingredients' category), and the pH was set at 5.7–5.8. [b]The number of regenerated shoots divided by the total number of explants after 4–6 weeks on the medium. [c]All explants are from diploid *T. porrifolius* (3078) seedlings, aged between 2 and 9 weeks; the explant number is calculated by summing across all replicates. [d]Pulse hormone treatment: the explants were placed on shooting medium for approximately 2 weeks for shoot initiation, and then the explants were placed on MS medium (4.44 g l^{-1} MS, 30 g l^{-1} sucrose, 5 g l^{-1} gelrite, pH 5.8) for approximately 3 weeks for shoot elongation. BAP, 6-benzylaminopurine; MS, Murashige & Skoog modified basal medium with Gamborg vitamins; NAA, α-naphthaleneacetic acid; TDZ, thidiazuron; WPM, Lloyd & McCown woody plant basal medium with vitamins; ZEA, *trans*-zeatin.

Table 2. Rooting media examined in *Tragopogon*

Medium[a]	Rooting rate (%)[b]	Hormones (mg l^{-1})	Other ingredients (g l^{-1})	Shoots[c] (replicates)
C3 pulse[d]	0	NAA (2.14), BAP (0.23)	MS (4.44), gelrite (5)	40 (5)
WPM-C3 pulse	59.0	NAA (2.14), BAP (0.23)	WPM (2.41), agargellan (8.5)	39 (4)
COCO-R pulse	56.0	IBA (1.5)	WPM (2.41), agargellan (8.5)	50 (5)
COCO-R2 pulse	65.9	NAA (2)	WPM (2.41), agargellan (8.5)	44 (4)

[a]All media contain 30 g l^{-1} sucrose (which is not listed in the 'Other ingredients' category), and the pH was set at 5.7–5.8. [b]The number of rooted shoots divided by the total number of shoots after approximately 3 weeks of treatment. [c]All shoots were regenerated from diploid *T. porrifolius* (3078) leaf explants; the shoot number is calculated by summing across all replicates. [d]Pulse hormone treatment: the shoots were placed on rooting medium for approximately 1 week, and then the shoots were transferred to either MS medium (4.44 g l^{-1} MS, 30 g l^{-1} sucrose, 5 g l^{-1} gelrite, pH 5.8) or WPM medium (2.41 g l^{-1} WPM, 30 g l^{-1} sucrose, 8.5 g l^{-1} agargellan, pH 5.7) for approximately 2 weeks. BAP, 6-benzylaminopurine; IBA, indole-3-butyric acid; MS, Murashige & Skoog modified basal medium with Gamborg vitamins; NAA, α-naphthaleneacetic acid; WPM, Lloyd & McCown woody plant basal medium with vitamins.

moved back to the growth chamber [14 h light (52.5 μmol m^{-2} s^{-1})/10 h dark, 25 °C], and after approximately 3–4 weeks, most plants began to bolt and flower.

Identification of the dihydroflavonol 4-reductase gene (*DFR*) in *Tragopogon*

The mRNA sequence from the *Lactuca sativa* (Asteraceae) *DFR* gene (XM_023893302.1) was used as a query to identify the *DFR* ortholog in *Tragopogon*. Using BLAST (version 2.8.1) (e-value cutoff: 1e-10), hits were identified from the *T. dubius* and *T. porrifolius* reference genome assemblies. The *DFR* genes in *T. dubius* and *T. porrifolius* were named *TduDFR* and *TpoDFR*, respectively. To predict the intron–exon structure and the coding sequence (CDS) of the candidate gene, exon sequences of *DFR* genes from model species were mapped to *TduDFR* and *TpoDFR* using the *Geneious* (11.0.5) mapper with default settings (except that the 'Sensitivity' parameter was set as 'Highest Sensitivity/Slow'); the model species we used in this step included: Arabidopsis (NM_123645.4), *Solanum lycopersicum* (XM_010317577.3), *Nicotiana tabacum* (XM_016626713.1), and *Helianthus annuus* (XM_022145746.1). The CDS of *TduDFR* and *TpoDFR* were then translated into amino acid sequences; the function of the derived proteins was predicted by using the InterPro database (version 5.66-98.0).

We also designed two sets of primers (i.e. TragDFR-F1 and TragDFR-R2, and TragDFR-F3 and TragDFR-R4; Supplementary Table S2) within conserved *DFR* regions across different species (including *Tragopogon* diploids and the model species described above); these same primer sets enabled amplification of the associated gene regions across different *Tragopogon* species. Using genomic DNAs from *T. porrifolius* (3078), *T. dubius* (3040-6-3), and *T. pratensis* (3058-1-2) as templates, the amplicons from these two sets of primers were genotyped using Sanger sequencing. Combining these sequencing results with the available genome

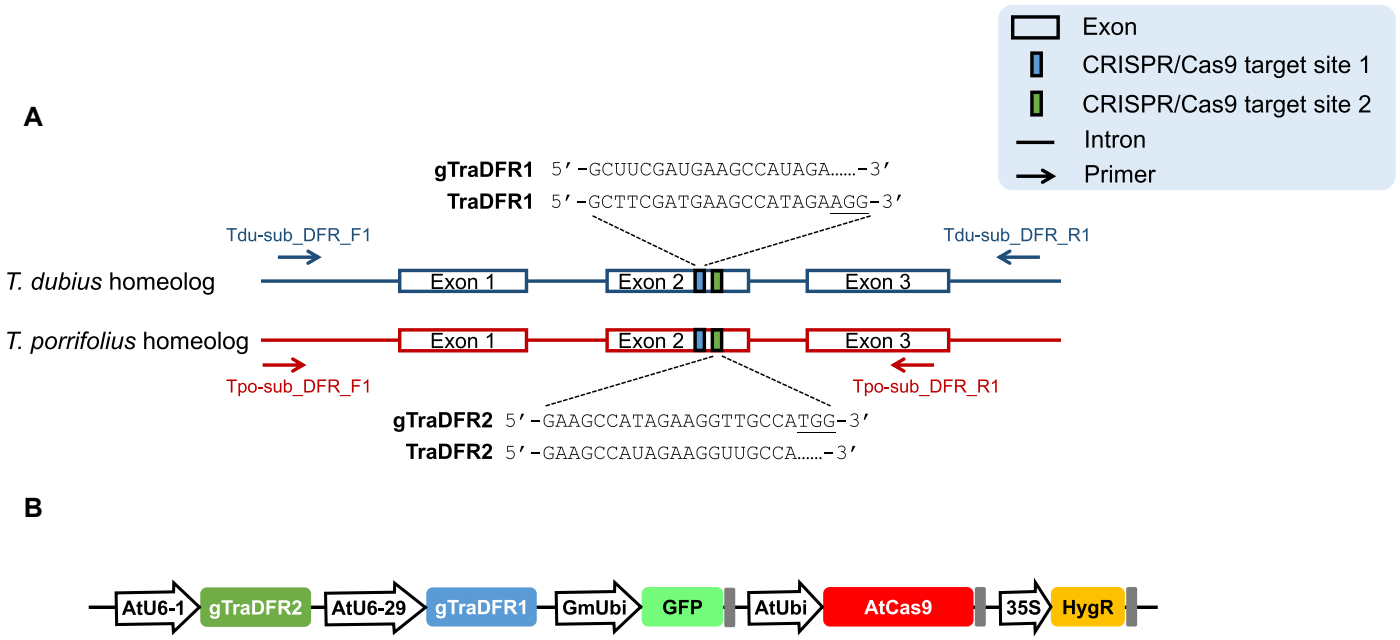

Fig. 1. The *Tragopogon DFR* gene and the strategy of creating a *DFR* knockout using CRISPR. (A) The two CRISPR/Cas9 target sites (located within exon 2) are conserved between the *T. dubius* homeolog and the *T. porrifolius* homeolog in allotetraploid *T. mirus*. sgRNA gTraDFR1 and gTraDFR2 were designed according to the sequences of CRISPR/Cas9 target sites TraDFR1 (i.e. target site 1) and TraDFR2 (i.e. target site 2), respectively. Protospacer adjacent motif sequences are underlined. Primers Tdu-sub_DFR_F1 and Tdu-sub_DFR_F2 were used to specifically amplify the *T. dubius* homeolog. The *T. porrifolius* homeolog was specifically amplified by using primers Tpo-sub_DFR_F1 and Tpo-sub_DFR_F2. (B) The CRISPR construct used for knocking out the *Tragopogon DFR* gene. Grey boxes represent terminators. Components are not drawn to scale. 35S, cauliflower mosaic virus *35S* promoter; AtCas9, codon-optimized *Cas9* gene for Arabidopsis; AtU6-1 and AtU6-29, two versions of Arabidopsis *U6* snRNA gene promoters; AtUbi, Arabidopsis *ubiquitin* promoter; GFP, *green fluorescent protein* gene; GmUbi, *Glycine max ubiquitin* promoter; HygR, hygromycin resistance gene.

assemblies, we identified two CRISPR/Cas9 target sites, i.e. TraDFR1 and TraDFR2, within the second exon of the *Tragopogon DFR* gene (Fig. 1A). In addition, the sequences at these two target sites are identical among all three diploid *Tragopogon* species that are parents of the North American allotetraploids, allowing the knockout of both homeologs in polyploid *Tragopogon* using the same sgRNA (described below).

Plasmid construction

The plasmid construction procedure follows protocols from Shan *et al.* (2018, 2023). Briefly, we started the cloning process with two constructs: pCAMBIA1300-Cas9-GFP (destination vector) and pENTR4-AtU6-1-AtU6-29 (entry vector). Based on the genomic sequences at the CRISPR/Cas9 target site TraDFR1, complementary oligonucleotides gTraDFR-F1 and gTraDFR-R1 were designed; we also designed gTraDFR-F2 and gTraDFR-R2 based on the sequence of TraDFR2 (Supplementary Table S2). Oligonucleotides gTraDFR-F1 and gTraDFR-R1 were annealed to generate double-stranded DNA oligonucleotides gTraDFR1; gTraDFR-F2 and gTraDFR-R2 were annealed to generate gTraDFR2. gTraDFR1 and gTraDFR2 were then integrated into the entry vector following AtU6-29 and AtU6-1 promoters, respectively (Fig. 1B). The final entry vector is named pENTR4-AtU6-1-gTraDFR2-AtU6-29-gTraDFR1.

The sgRNA cassette from the entry vector was then mobilized into the destination vector through the Gateway LR reaction (Thermo Fisher Scientific, Waltham, MA, USA). The final plasmid is named pCAMBIA1300-Cas9-GFP-AtU6-1-gTraDFR2-AtU6-29-gTraDFR1 (Fig. 1B), which has been confirmed through whole plasmid sequencing (performed by Plasmidsaurus using Oxford Nanopore Technology). We then transformed *Agrobacterium tumefaciens* strain EHA105 with the final plasmid using electroporation.

Genotyping putative genome-edited *T. porrifolius* and *T. mirus*

First, we tested to determine whether the transgene (i.e. the CRISPR cassette) is integrated into the genomes of the regenerated *T. porrifolius* and *T. mirus* plants. Primers AtU6-F2 and AtU6-R2 were used to amplify a DNA fragment (476 bp) within the AtU6-29 promoter, which is part of the transfer DNA (T-DNA) (Supplementary Table S2). Genomic DNAs from regenerated plants were extracted following a modified cetyltrimethylammonium bromide (CTAB) protocol (Doyle and Doyle, 1987). One microliter of genomic DNA (25–125 ng) was added into a 25 µl PCR system, including 1× Green Go Taq Reaction Buffer (Promega, Madison, WI, USA), 2.5 mM $MgCl_2$, 200 µM dNTPs, 0.5 µM of each primer, and 0.05 U μl^{-1} Apex *Taq* DNA polymerase (Genesee Scientific, El Cajon, CA, USA). The PCR conditions were as follows: one cycle of denaturation at 95 °C for 3 min; 32 cycles at 95 °C for 30 s, 68.1 °C annealing for 30 s, and 72 °C extension for 1 min; one cycle at 72 °C for 5 min; and hold at 4 °C. A plant was classified as transgenic when a band of the anticipated size (476 bp) was detected through gel electrophoresis.

Second, we genotyped the *DFR* gene in regenerated *T. porrifolius* and *T. mirus* individuals. To genotype *T. porrifolius*, primers TragDFR-F1 and TragDFR-R2 were used to amplify a fragment (containing the CRISPR target sites) from *TpoDFR*. One microliter of genomic DNA (20–100 ng) was added into a 20 µl PCR [1× Phusion HF Buffer (New England Biolabs, Ipswich, MA, USA), 200 µM dNTPs, 0.5 µM of each primer, 0.02 U μl^{-1} Phusion DNA polymerase (New England Biolabs)]. The

PCR conditions were as follows: one cycle of denaturation at 98 °C for 30 s; 32 cycles at 98 °C for 10 s, 59.5 °C annealing for 30 s, and 72 °C extension for 1 min 15 s; one cycle at 72 °C for 10 min; and hold at 4 °C. The PCR product was accessed via gel electrophoresis; the band with the expected size (~1.7 kb) was excised from the gel and purified using the Wizard *Plus* SV Minipreps DNA Purification System (Promega). PCR products were then sequenced at Eurofins Genomics (Louisville, KY, USA), and the genotypes were deciphered from the sequencing chromatograms using the method described in Shan *et al.* (2018).

For *T. mirus*, we genotyped one homeolog at a time. Utilizing the SNP and indel differences between the two homeologs of *DFR* in *T. mirus*, we used *GSP* (Wang *et al.*, 2016) to design homeolog-specific primers: Tdu-sub_DFR_F1 and Tdu-sub_DFR_R1 were used to amplify the *T. dubius* homeolog (amplicon size: 992 bp), and Tpo-sub_DFR_F1 and Tpo-sub_DFR_R1 were used to amplify the *T. porrifolius* homeolog (amplicon size: 851 bp) (Fig. 1A; Supplementary Table S2). To amplify each homeolog in *T. mirus*, the PCR conditions were the same as described above (for genotyping *T. porrifolius*) except for the annealing temperature and extension time. For both sets of primers, the annealing temperature was 61.5 °C, and the PCR extension time was 45 s. PCR products were then purified and sequenced, and the genotypes were determined from the sequencing chromatograms as described above.

Results

Shoot and root regeneration of *Tragopogon* on various media

The results of regenerating *T. porrifolius* shoots from various media are shown in Table 1. Among the 11 different shooting media, COCO-1 medium (with pulse hormone treatment) led to the highest shooting rate: 40.9% (Table 1). In addition, little or no hyperhydricity was observed in regenerated shoots from the COCO-1 pulse hormone treatment (Supplementary Fig. S1). Placing the explants continuously on COCO-1 medium led to a shooting rate of 8.6%. On the other hand, pulse hormone treatment of C3 medium showed a 0% shooting efficiency (Table 1). Additionally, the shooting rate on COCO medium was 1.1% (Table 1). The only difference between COCO and COCO-1 media was the source of salt: MS and WPM salts were used in COCO and COCO-1 media, respectively; these results showcased the effect of salt type (i.e. different concentrations of macro- and micronutrients) on shoot regeneration (Table 1). Using IA-7 and SIM media also resulted in a relatively high shooting efficiency: the shooting rates were 9.0% and 9.6% on IA-7 and SIM media, respectively (Table 1). Lastly, many media showed a 0% shooting efficiency in *Tragopogon* (Table 1), although all tested media were adapted from established protocols from species in Asteraceae (Mechanda *et al.*, 2003; Hunter and Burritt, 2004; Trigiano *et al.*, 2011; Armas *et al.*, 2017).

We tested four rooting media using the regenerated shoots from *T. porrifolius* (Table 2). All media adopted the pulse hormone treatment approach given its success in inducing shoot regeneration (see above). C3 and WPM-C3 media resulted in 0% and 59.0% rooting rate, respectively (Table 2). With IBA as the source of auxin, COCO-R had a rooting rate of 56.0%; COCO-R2 (containing 2 mg l^{-1} NAA) also led to a high rooting rate (65.9%; Table 2). All regenerated roots showed normal morphology (Supplementary Fig. S1).

In addition, the regenerated *T. porrifolius* seedlings (with both shoots and roots) bolted and flowered after 3 months of cold treatment. The average pollen stainability was 70.6%, indicating high pollen fertility in regenerated *T. porrifolius* plants (Supplementary Table S3; Supplementary Fig. S1). Seeds from the regenerated *T. porrifolius* were successfully germinated, with an average germination rate of 78.4% (Supplementary Table S3). Lastly, we found that the regeneration system developed for *T. porrifolius* was also effective in *T. mirus* (Supplementary Fig. S2), demonstrating the broad applicability of our current system.

Characterization of the *Tragopogon DFR* gene

Using the assembled *Tragopogon* genomes, we obtained the *DFR* sequences of the diploid species: *T. dubius* (*TduDFR*), *T. porrifolius* (*TpoDFR*), and *T. pratensis* (*TprDFR*). Using the *Lactuca* DFR (AVV62509.1) amino acid sequence as the query, a single best hit (>80% of identical matches and >300 aa alignment length) was found in each of the three diploids, suggesting that there is only one copy of *DFR* in diploid *Tragopogon* genomes (Supplementary Table S4). In all diploids, there are six exons in *DFR*, and the length of the CDS is 1077 bp. The number of single-nucleotide polymorphisms (SNPs) within the *DFR* CDS is 16, 14, and four between *T. dubius* and *T. porrifolius*, *T. dubius* and *T. pratensis*, and *T. porrifolius* and *T. pratensis*, respectively. InterPro predicted that the *Tragopogon* DFR contains the NAD-dependent dehydratase domain (IPR001509), which is highly conserved among *DFR* genes from various plant species (Li *et al.*, 2023).

Genome-editing of *DFR* in diploid *T. porrifolius*

Following *Agrobacterium*-mediated transformation, the percentage of explants with transgenic events was 74.4%, indicating a high transformation efficiency (Table 3). The shooting and rooting rates in *T. porrifolius* were 11.3% and 33.3%, respectively (Table 3). We obtained five regenerated *T. porrifolius* individuals with both shoots and roots and genotyped four plants that survived the cultivation process (i.e. D07-1, D07-2, D07-3, and D07-5) (Fig. 2; Table 3). We confirmed the integration of the transgene into the genomes of all four individuals (Fig. 2A). In all four transgenic *T. porrifolius* plants, both *DFR* alleles were successfully edited (Fig. 2B; Table 3). All edits consisted of deletions of a few nucleotides. For example, individual D07-1 had 8 bp and 13 bp deletions, while 14 bp and 15 bp deletions were found in plant D07-2 (Fig. 2B).

In addition, we confirmed the inheritance of *DFR* mutations in the T_1 generation. Genotypes of two *T. porrifolius* T_1 individuals, D07-2-1 (the progeny of D07-2) and D07-3-1 (the progeny of D07-3), were examined. Transgenes were found in both T_1 progenies (Supplementary Fig. S3A). Plant

Table 3. The statistics of the plant transformation study in *T. porrifolius* (2*x*) and *T. mirus* (4*x*)

Species	Explants	Explants with transgenic events[a]	Regenerated shoots[b]	Rooted shoots[c]	Genotyped plants	Transgenic plants	Plants with all alleles edited[e]
T. porrifolius	133	99 (74.4%)	15 (11.3%)	5 (33.3%)	4[d]	4	4 (100%)
T. mirus	102	90 (88.2%)	38 (37.3%)	9 (23.7%)	9	7	5 (71.4%)

[a]Explants that developed hygromycin-resistant calli with green fluorescent protein signal were considered successfully transformed; transformation efficiency (indicated as a percentage) was calculated by dividing the number of explants with transgenic events by the total number of explants. [b]Number of regenerated shoots moved to the rooting medium; shooting rate (the percentage following the shoot number) was determined by dividing the number of regenerated shoots by the total number of explants. [c]Number of rooted shoots moved to soil; rooting rate, shown as the percentage following the number of rooted shoots, was calculated by dividing the number of rooted shoots by the shoot number. [d]Not all rooted shoots were genotyped, as one plant died during the cultivation process. [e]These plants include *T. porrifolius*, which had two edited alleles, and *T. mirus*, which had four edited alleles; the percentage following the plant number was calculated by dividing the number of plants with all alleles edited by the total number of transgenic plants.

D07-2-1 inherited the two mutant alleles (i.e. 14 bp and 15 bp deletions) from D07-2 (Supplementary Fig. S3B). Individual D07-3 had a homozygous *DFR* mutation (5 bp deletion) (Fig. 2B), and the same mutant allele was also homozygous in D07-3-1 (Supplementary Fig. S3B).

In terms of phenotypes, the *T. porrifolius dfr* mutants had green leaves without anthocyanin pigmentation (Fig. 3). In addition, the mutants had white ligules, in contrast to the purple ligules found in wild-type plants, indicating the absence of anthocyanin (Fig. 3). Seven of the eight *DFR* alleles from the four transgenic *T. porrifolius* individuals contained frame-shift mutations (Fig. 2B). One allele of individual D07-2 had a 15 bp deletion, which leads to an in-frame mutation with a preserved reading frame (Fig. 2B). The five deleted amino acids (position 73–77) are located within the NAD-dependent dehydratase domain (position 9–250), which is characteristic of DFR proteins. The absence of these amino acids may impair the function of the DFR protein, which may explain the lack of the anthocyanin phenotype observed in the leaf and inflorescence tissues of D07-2 (Fig. 3).

Genome-editing of *DFR* in tetraploid *T. mirus*

For *T. mirus*, we obtained nine regenerated plants with both shoots and roots following *Agrobacterium*-mediated transformation (Fig. 2C; Table 3). The transformation efficiency was 88.2%, and the shooting and rooting efficiencies were 37.3% and 23.7%, respectively (Table 3). All nine plants were genotyped. The transgene was integrated into the genomes of all *T. mirus* individuals except D13-5 and D13-7 (Fig. 2A); these two plants escaped multiple rounds of hygromycin selection during the tissue culture process. Next, we genotyped the *DFR* gene in these plants by individually sequencing the subgenome-specific amplicons (one from the *T. dubius*-derived subgenome and the other from the *T. porrifolius*-derived subgenome) of the gene. Primers Tdu-sub_DFR_F1 and Tdu-sub_DFR_R1 specifically amplified the *T. dubius* homeolog in *T. mirus*; no amplicon was detected when the *T. porrifolius* genomic DNA was used as the template for PCR (Supplementary Fig. S4A). Primers Tpo-sub_DFR_F1 and Tpo-sub_DFR_R1 specifically amplified the *T. porrifolius* homeolog in *T. mirus*, as confirmed by the absence of the amplicon in the *T. dubius* individual (Supplementary Fig. S4B). In addition, sequencing results showed that diagnostic SNPs and indels differentiating *T. dubius* and *T. porrifolius DFR* genes were also found between the amplicons derived from each subgenome in *T. mirus*, further confirming the specificity of the primers (Fig. 2C).

The two non-transgenic individuals (D13-5 and D13-7), as expected, both had the wild-type alleles (Fig. 2C). All seven transgenic plants had at least one *DFR* allele edited: five (71.4%) had all four *DFR* alleles edited, and plants D13-1 and D13-9 had one and three alleles modified, respectively (Fig. 2C; Table 3). Most edited alleles contained small indels (<15 bp), except for two large deletions (39 bp and 97 bp) found in plant D13-10 (Fig. 2C). Deletions (13 of 20 edited alleles) were more prevalent than insertions (7 of 20 edited alleles), with all insertion events adding a single nucleotide to the target gene at the same position (Fig. 2C). In addition, there was no observed editing bias between the two homeologs: 13 *T. dubius* homeologs and 11 *T. porrifolius* alleles were edited. This result is expected because the CRISPR target sites are located within conserved sequences between homeologs.

Phenotypes of three *T. mirus* individuals, D13-2, D13-4, and D13-5, are shown in Fig. 4. The non-transgenic, and therefore non-edited, plant D13-5 exhibited the wild-type phenotype with purple ligules and anthocyanin pigment in leaves (Fig. 4). Individual D13-4, with all four *DFR* alleles edited, did not accumulate anthocyanin throughout the plant (Fig. 4). Moreover, the ligule color of D13-4 was yellow, indicating that knocking out *DFR* disrupted the anthocyanin biosynthesis pathway but did not affect the pathway synthesizing yellow carotenoids in the inflorescence (Fig. 4). For plant D13-2, the genotyping result showed that all four alleles were modified (Fig. 2C). However, anthocyanin pigment was found in leaf tissues, and the ligule color was light purple

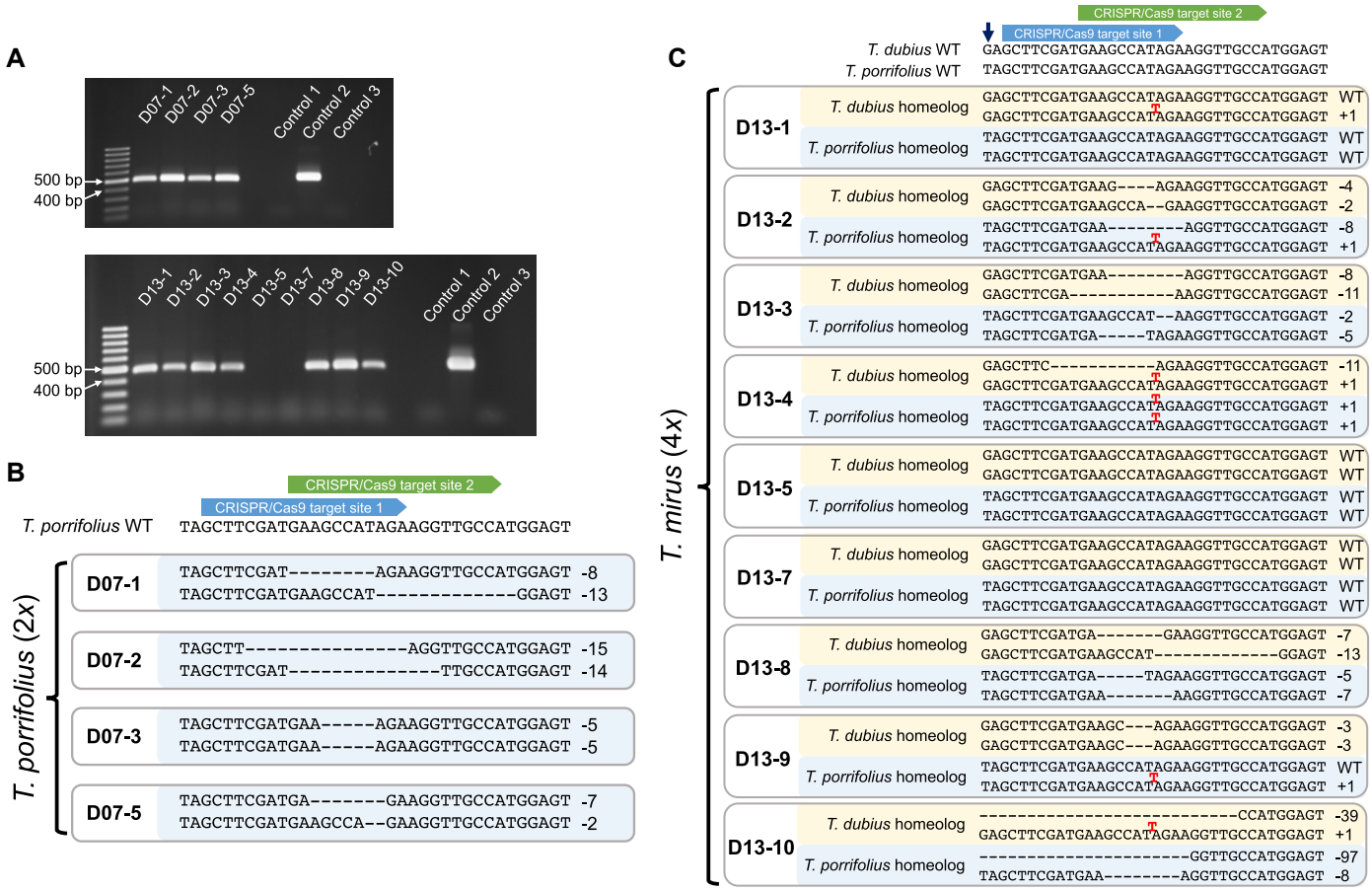

Fig. 2. Genome editing results in *T. porrifolius* (2*x*) and *T. mirus* (4*x*). (A) PCR followed by gel electrophoresis was employed to examine the presence of the transgene in *T. porrifolius* (D07) and *T. mirus* (D13) individuals. Primers AtU6-F2 and AtU6-R2 were used to amplify a DNA fragment (476 bp), which is part of the transfer DNA. Control 1 (negative control) used the DNA from a wild-type *T. porrifolius* individual (i.e. B54-1-5) or a wild-type *T. mirus* as the template; control 2 (positive control) used the plasmid DNA from pCAMBIA1300-Cas9-GFP-AtU6-1-gTraDFR2-AtU6-29-gTraDFR1 as the template; control 3 (negative control) lacks DNA template. (B) Genotypes of the four *T. porrifolius* individuals. Sequences at the two CRISPR/Cas9 target sites are shown. (C) Genotypes of the nine *T. mirus* individuals. Sequences at the two CRISPR/Cas9 target sites are shown, and the single nucleotide polymorphism between *T. dubius* and *T. porrifolius* wild types is indicated by the arrow. Red letters present nucleotide insertions. For individual D13-10, not all the deleted nucleotides in the '–39' and '–97' alleles are shown. '–*x*' denotes an *x* bp deletion (i.e. 4, 2, 8 bp, etc.); '+*y*' indicates a *y* bp insertion (i.e. 1 bp). WT, wild type.

(Fig. 4). The weak anthocyanin accumulation observed in D13-2 was probably from a negligible portion of the mosaic tissues carrying the functional alleles (e.g. the wild-type allele), despite the prevalence of the four frame-shift mutated alleles proportionally PCR-amplified and detected by Sanger sequencing. Indeed, while Sanger sequencing of PCR amplicons can determine predominant allele types, it is not capable of identifying rare editing events (Shan *et al.*, 2020b). Future studies could use high-throughput deep sequencing to identify all rare genome editing events in this plant. Lastly, comparing phenotypes and genotypes of these three *T. mirus* individuals suggests that anthocyanin quantity increases with a higher dosage of *DFR* wild-type alleles. A more systematic study with mutants having varying numbers of mutated *DFR* alleles (e.g. one, two, three, and four) is required to confirm this interpretation.

Discussion

Development of an efficient regeneration system in non-genetic model plants

Although CRISPR itself is an efficient and easy-to-use genome editing approach, the difficulty of developing efficient transformation and regeneration systems in non-genetic model plants prevents the broad application of CRISPR (Altpeter *et al.*, 2016; Shan *et al.*, 2020b). In our initial work on developing a tissue culture system in *Tragopogon*, four shooting media were tested, and nine explants were examined for each medium (Shan *et al.*, 2018). Although the highest shooting rate reached 38.9%, the prevalence of hyperhydricity in regenerated shoots and the lack of a rooting system impeded the regeneration of plants with both shoots and roots, which are essential for nearly all gene functional studies (Shan *et al.*, 2018). In the

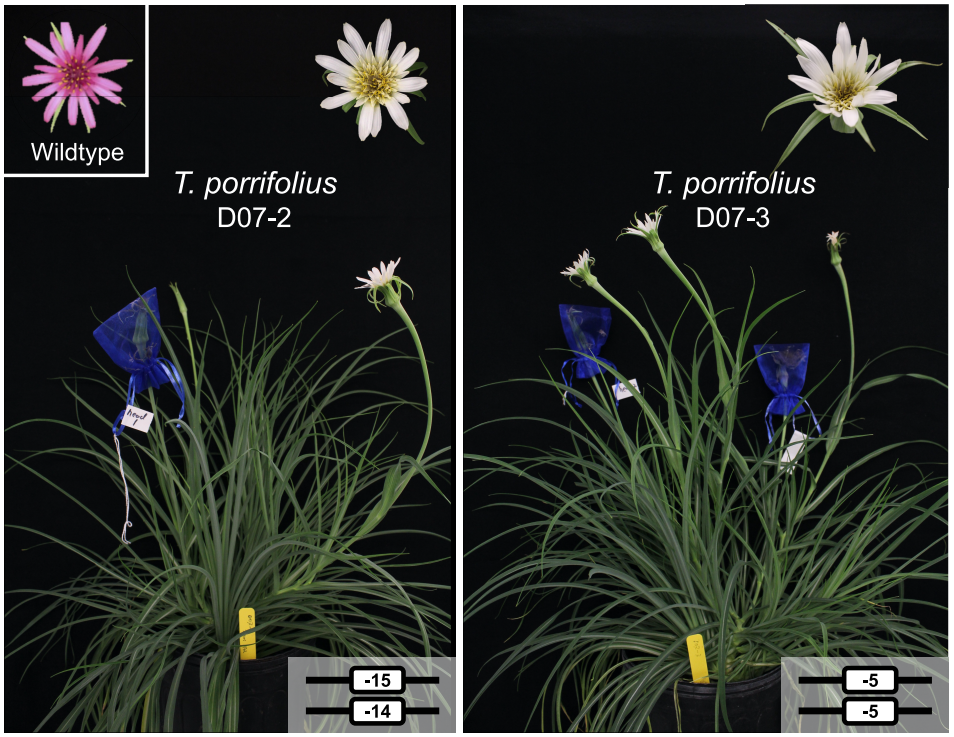

Fig. 3. Phenotypes and genotypes of *T. porrifolius dfr* mutants. Two genome-edited plants, D07-2 and D07-3, are shown here. The purple wild-type inflorescence of *T. porrifolius* is displayed in the upper-left corner. For each plant, a representative inflorescence is shown in the upper right, with the genotype indicated in the lower right ('−14' denotes a 14 bp deletion; each line represents one allele). The ligule color was white for both *dfr* mutants, and the leaves did not accumulate anthocyanin. T_1-generation achenes were collected in blue mesh bags.

present work, compared with Shan *et al.* (2018), more media (11) and explants (median: 116 explants per medium) were examined for shoot regeneration (Table 1), and four different rooting media were tested for the first time in *Tragopogon* (Table 2). The highest shooting rate was 40.9% when the explants were placed on the COCO-1 medium with pulse hormone treatment (Table 1), and the regenerated shoots had normal morphology without hyperhydricity (Supplementary Figs S1, S2). Additionally, three of the four rooting media resulted in a high rooting rate (56.0–65.9%; Table 2).

To develop a tissue culture system in a non-genetic model plant, adapting methods from phylogenetically closely related species serves as a reliable reference and a reasonable starting point (Birch, 1997; Shan *et al.*, 2020b). The COCO-1 medium was adapted from the shooting medium used in *Echinacea purpurea* (Asteraceae), in which coconut water and WPM salt were used (Mechanda *et al.*, 2003). Importantly, neither of these two components was present in the original shooting medium described in Shan *et al.* (2018), which consisted of 4.44 g l^{-1} MS salts, 0.4 mg l^{-1} BAP, and 6 g l^{-1} agargellan (pH 5.8). Below, we discuss the potential roles of coconut water and WPM salts in enhancing regeneration efficiency and reducing hyperhydricity.

Coconut water, the aqueous part of the coconut endosperm, has been widely used as a growth supplement in plant tissue culture due to its unique composition of sugars, vitamins, minerals, amino acids, and hormones (Yong *et al.*, 2009). Coconut water contains various types of cytokinins, including *trans*-zeatin riboside, *trans*-zeatin, kinetin, and kinetin riboside, which promote shoot regeneration (Van Staden and Drewes, 1975; Ge *et al.*, 2005; Yong *et al.*, 2009; Ikeuchi *et al.*, 2016). Other hormones, including auxin, gibberellins, and abscisic acid, have also been identified in coconut water (Yong *et al.*, 2009).

In terms of the impact of salt type on plant regeneration, WPM salt greatly improved shoot and root regeneration in *Tragopogon* compared with MS salt. Using MS salt, COCO medium led to a shooting rate of 1.1%. In contrast, with all ingredients unchanged except for using WPM salt, COCO-1 medium resulted in a shooting rate of 8.6% (Table 1). Similarly, the rooting rates were 0% and 59.0% for C3 medium and WPM-C3 medium, respectively; the only difference between the two media is that C3 medium used MS salt, while WPM-C3 medium contained WPM salt (Table 2). Both MS salt and WPM salt are widely used for plant tissue culture, and the primary difference between the two is that WPM contains less total nitrogen (15 mM vs. 60 mM) and less ammonium (5 mM vs. 20 mM) compared with MS (Murashige and Skoog, 1962; Lloyd and McCown, 1980; Phillips and Garda, 2019; Long *et al.*, 2022). As observed in *Tragopogon*, reducing

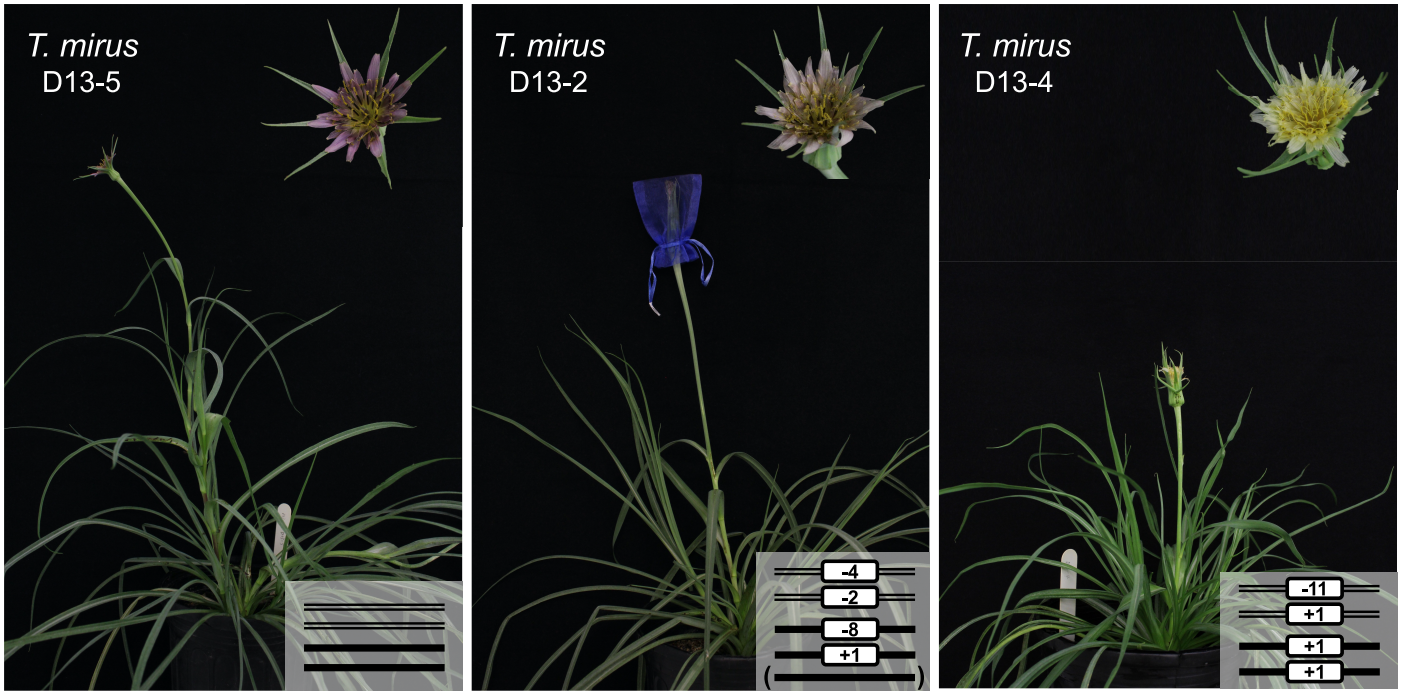

Fig. 4. Phenotypes and genotypes of unedited and edited *T. mirus* individuals. For each plant, a representative inflorescence is shown in the upper right, with the genotype indicated in the lower right ('−4' denotes a 4 bp deletion; '+1' indicates 1 bp insertion; the doubled and solid lines represent alleles from the *T. dubius* homeolog and the *T. porrifolius* homeolog, respectively). All four alleles of the *DFR* gene in D13-5 were unedited. Edits were found in the four predominant allele types in D13-2, and the wild-type allele (indicated by the solid line in parentheses) may be present in a small portion of cells in this plant. All four alleles were edited in D13-4. T_1-generation achenes were collected in blue mesh bags.

the amount of nitrogen in the medium promotes plant regeneration and growth in some plant species, including potato (Avila *et al.*, 1998) and *Senecio* (Gertsson, 1988). In contrast, a higher level of nitrogen led to a better regeneration result in *Aloe* (Ivanova and Van Staden, 2009) and *Helianthus* (Knittel *et al.*, 1991). These results indicate that the effect of nitrogen concentration on plant regeneration varies significantly among different species, and both MS and WPM salts should be tested to find the optimal nitrogen concentration for a non-genetic plant model. In addition, compared with WPM salt, MS salt has a higher ammonium concentration, which may cause ammonium toxicity (Phillips and Garda, 2019) and inhibit availability of mineral nutrients to the plant (Ramage and Williams, 2002). Moreover, in many species, reducing the concentration of ammonium lowers the level of hyperhydricity (Polivanova and Bedarev, 2022). Therefore, the lack of hyperhydricity in *Tragopogon* shoots regenerated on COCO-1 medium may be due to the low ammonium concentration in the WPM salt (Supplementary Figs S1, S2).

The duration of hormone exposure affects plant regeneration, and prolonged hormone treatment can lead to unintended developmental outcomes (George *et al.*, 2008; Dewir *et al.*, 2018). For example, in *Psophocarpus* (Fabaceae), 1 week of hormone exposure resulted in 100% of explants forming shoot buds, whereas 25 d of exposure led to only 40% (Hanh *et al.*, 1981). In *Helianthus annuus*, minimizing the duration of hormone exposure on shooting medium reduced callus production and improved shoot development (Baker *et al.*, 1999). In terms of rooting, James and Wakerell (1982) found that prolonged exposure to auxin decreased the regenerated root number in apple shoots. Similarly, in *Tragopogon*, continuous hormone treatment for 5 weeks on COCO-1 medium resulted in a shooting rate of 8.6%. However, a pulse hormone treatment for 2 weeks on COCO-1 medium, followed by 3 weeks on a hormone-free MS medium, increased the shooting rate to 40.9% (Table 1). In addition, a 1 week hormone treatment followed by a 2 week period on a hormone-free medium led to a high rooting rate in *Tragopogon* (Table 2). Indeed, in many species, the shooting process involves an initial shoot initiation phase on a hormone-containing medium, followed by a shoot elongation phase on a hormone-free medium (Wang *et al.*, 2007; Trigiano *et al.*, 2011; Zaytseva *et al.*, 2020). The use of hormone-free medium following pulse auxin exposure has also been widely adopted for root regeneration in various species (Lu *et al.*, 1991; Husain *et al.*, 2008; Jahan *et al.*, 2011).

Lastly, *Agrobacterium*-mediated transformation may negatively impact plant regeneration. *Agrobacterium* inoculation can cause plant tissue browning and necrosis (Altpeter *et al.*,

2016). In addition, plant growth and regeneration can be affected by the addition of antibiotics in the culture medium, which are used for the selection of transformed cells and the elimination of excessive *Agrobacterium* (Nauerby *et al.*, 1997; Ziemienowicz, 2014; Sabbadini *et al.*, 2019). In *T. porrifolius*, without *Agrobacterium*-mediated transformation, the shooting and rooting rates were 40.9% and 56.0%, respectively (Tables 1, 2). In contrast, following transformation and the addition of antibiotics in the regeneration media (15 mg l^{-1} hygromycin and 300 mg l^{-1} timentin), the shoot and root regeneration rates decreased to 11.3% and 33.3%, respectively (Table 3). The reduced regeneration rates may result from the combined effects of *Agrobacterium* inoculation and antibiotic selection. Without additional data, we cannot assess the independent effect of *Agrobacterium* on *Tragopogon* regeneration, which is worth exploring in future studies.

Although *Tragopogon* regeneration was affected by the transformation process, the straightforward and fast nature of plant regeneration alone allowed for the testing of many media for shooting and rooting in *Tragopogon* without the prolonged *Agrobacterium* infection and transformant selection procedures. This same approach—establishing the regeneration protocol first and then applying the transformation process—can be adopted in other non-genetic models, as demonstrated here for *Tragopogon* and in many other plant systems, including lettuce (*Lactuca sativa*) (Mohebodini *et al.*, 2011, 2014), dogwood (*Cornus canadensis*) (Liu *et al.*, 2013), bamboo (*Dendrocalamus latiflorus*) (Ye *et al.*, 2017), and grapevine (*Vitis* spp.) (Sabbadini *et al.*, 2019).

Genome editing in polyploids

Although the presence of multiple copies of target genes makes genome editing in polyploids challenging, CRISPR-mediated editing has been widely applied in polyploid species, particularly in crops. As reviewed by May *et al.* (2023), genome editing techniques have been applied in more than 20 polyploid plant species. For example, CRISPR/Cas9 was used to edit the banana streak virus integrated into the B subgenome of triploid plantain cultivar Gonja Manjaya (Tripathi *et al.*, 2019). Using multiple sgRNAs, the editing efficiency reached 95%. The resulting genome-edited germplasm represents a valuable resource for future breeding programs (Tripathi *et al.*, 2019). In tetraploid potato (*Solanum tuberosum*), CRISPR/Cas9 was used to reduce enzymatic browning following cutting (González *et al.*, 2020); the CRISPR construct was designed to target the polyphenol oxidase gene *StPPO2*. Ribonucleoprotein complexes (composed of sgRNAs and Cas9) were transfected into potato protoplasts, resulting in 68% of regenerated plants having at least one edited *StPPO2* allele, and 24% of edited lines carrying mutations in all four alleles (González *et al.*, 2020). CRISPR/Cas9 was successfully used to knock out a fruit coloration gene (*RAP*) in octoploid strawberry (*Fragaria*×*ananassa*) (Gao *et al.*, 2020). The *RAP* gene has six copies from three of the four homeologous chromosomes. Using two sgRNAs, Gao *et al.* (2020) generated mutant lines in which all six copies were edited in the T_0 generation, paving the way for future fruit color breeding of strawberry. In tetraploid rapeseed (*Brassica napus*), four copies of the *BnaEOD3* gene have been identified (Khan *et al.*, 2021). CRISPR/Cas9-mediated genome editing generated quadruple mutants—with all four copies edited—in the T_1 generation. These mutants exhibited a 13.9% increase in seed weight per plant compared with wild-type *B. napus* (Khan *et al.*, 2021). Highly efficient genome editing has been achieved in both tetraploid durum wheat (*Triticum turgidum*) and hexaploid bread wheat (*T. aestivum*). Komura *et al.* (2025) employed a CRISPR/Cas9 platform utilizing a tRNA processing system to simultaneously express six sgRNAs targeting the *PCL1* gene, a flowering time regulator. Remarkably, all homeologs of the target gene were edited in the T_0 generation, with an editing efficiency of 100% in both tetraploid and hexaploid wheat (Komura *et al.*, 2025).

Most CRISPR studies in polyploids have focused on domesticated crop species, while naturally occurring polyploids remain largely unstudied. In the current work, the improved transformation and regeneration system in *Tragopogon* allows the development of an efficient CRISPR/Cas9 platform in this evolutionary model for studies of recent and recurring polyploidy. In allotetraploid *T. mirus*, all transgenic T_0 individuals had at least one mutant *DFR* allele, and 71.4% of T_0 individuals had all four *DFR* alleles edited (Fig. 2C; Table 3). Genotyping results of T_1-generation individuals indicated that edits were heritable in *Tragopogon* (Supplementary Fig. S3). In addition, anthocyanin pigmentation was absent in *T. porrifolius* and *T. mirus* mutants that had only mutant alleles encoding non-functional DFR (Figs. 3, 4).

Summary

We have developed a highly efficient genetic transformation and CRISPR/Cas9 system in *Tragopogon*. Utilizing the efficient CRISPR/Cas9 platform in recently formed polyploid *Tragopogon mirus*, we will be able to elucidate the genetic basis of complex traits following WGD and the consequences of WGD on those traits. In addition to the broader relevance with respect to polyploidy, the efficient genome editing platform in *Tragopogon* will also provide insights into the origin and evolution of complex traits in Asteraceae. As one example, this work paves the way for study of the unique inflorescence—the head or capitulum—that characterizes the entire Asteraceae, the largest angiosperm family (~25,000 species; Judd *et al.*, 2016). The methods and approaches used, as well as the challenges faced in building this platform, also provide a framework for other researchers hoping to build similar systems for other evolutionary models in other groups that are not genetic models.

Supplementary data

The following supplementary data are available at *JXB* online.

Fig. S1. The regeneration process in *T. porrifolius*.

Fig. S2. The regeneration process in *T. mirus*.

Fig. S3. Genome editing results in *T. porrifolius* (2*x*) T_1 generation.

Fig. S4. *Tragopogon mirus DFR* homeolog amplification using homeolog-specific primers.

Table S1. Media for *Agrobacterium*-mediated transformation and regeneration in *Tragopogon*.

Table S2. Sequences of primers used in this study.

Table S3. Pollen stainability of regenerated *T. porrifolius*.

Table S4. The best blastp hits in *Tragopogon* diploids using the *Lactuca* DFR amino acid sequence as query.

Acknowledgements

The authors thank Christopher Dervinis, Hua Liu, and Bo Liu for helpful discussion.

Author contributions

DES, BY, PSS, WBB, and SS designed the project. SS performed the research with help from MTP, ZZ, EVM, MAG, and BAH. SS, DES, BY, PSS, CEG, and WBB wrote the manuscript. All authors reviewed and approved the manuscript.

Conflict of interest

The authors declare they have no conflicts of interest.

Funding

This work was supported by US National Science Foundation grants IOS-1923234 to DES, PSS, BY, and WBB, and DEB-2043478 to DES and PSS.

Data availability

mRNA sequences of *DFR* from *T. dubius* (*TduDFR*), *T. porrifolius* (*TpoDFR*), and *T. pratensis* (*TprDFR*) have been submitted to GenBank (Accession numbers PP916141, PP916142, and PP916143, respectively). Sequencing results of *DFR* from *T. porrifolius* and *T. mirus* mutants have been uploaded to Dryad (Shan *et al.*, 2024b). The protocol is available at protocols.io: dx.doi.org/10.17504/protocols.io.e6nvwbo5zvmk/v1.

References

Altpeter F, Springer NM, Bartley LE, *et al.* 2016. Advancing crop transformation in the era of genome editing. The Plant Cell **28**, 1510–1520.

Armas I, Pogrebnyak N, Raskin I. 2017. A rapid and efficient *in vitro* regeneration system for lettuce (*Lactuca sativa* L.). Plant Methods **13**, 58.

Avila AL, Pereyra SM, Argüello JA. 1998. Nitrogen concentration and proportion of NH_4^+-N affect potato cultivar response in solid and liquid media. HortScience **33**, 336–338.

Baker CM, Muñoz-Fernandez N, Carter CD. 1999. Improved shoot development and rooting from mature cotyledons of sunflower. Plant Cell, Tissue and Organ Culture **58**, 39–49.

Birch RG. 1997. Plant transformation: problems and strategies for practical application. Annual Review of Plant Biology **48**, 297–326.

Birchler JA, Veitia RA. 2007. The gene balance hypothesis: from classical genetics to modern genomics. The Plant Cell **19**, 395–402.

Birchler JA, Veitia RA. 2012. Gene balance hypothesis: connecting issues of dosage sensitivity across biological disciplines. Proceedings of the National Academy of Sciences, USA **109**, 14746–14753.

Blanc G, Wolfe KH. 2004. Functional divergence of duplicated genes formed by polyploidy during *Arabidopsis* evolution. The Plant Cell **16**, 1679–1691.

Boatwright JL, McIntyre LM, Morse AM, Chen S, Yoo MJ, Koh J, Soltis PS, Soltis DE, Barbazuk WB. 2018. A robust methodology for assessing differential homeolog contributions to the transcriptomes of allopolyploids. Genetics **210**, 883–894.

Buggs RJ, Zhang L, Miles N, Tate JA, Gao L, Wei W, Schnable PS, Barbazuk WB, Soltis PS, Soltis DE. 2011. Transcriptomic shock generates evolutionary novelty in a newly formed, natural allopolyploid plant. Current Biology **21**, 551–556.

Buggs RJ, Chamala S, Wu W, Tate JA, Schnable PS, Soltis DE, Soltis PS, Barbazuk WB. 2012. Rapid, repeated, and clustered loss of duplicate genes in allopolyploid plant populations of independent origin. Current Biology **22**, 248–252.

Chaudhary B, Flagel L, Stupar RM, Udall JA, Verma N, Springer NM, Wendel JF. 2009. Reciprocal silencing, transcriptional bias and functional divergence of homeologs in polyploid cotton (*Gossypium*). Genetics **182**, 503–517.

Chester M, Gallagher JP, Symonds VV, Cruz da Silva AV, Mavrodiev EV, Leitch AR, Soltis PS, Soltis DE. 2012. Extensive chromosomal variation in a recently formed natural allopolyploid species, *Tragopogon miscellus* (Asteraceae). Proceedings of the National Academy of Sciences, USA **109**, 1176–1181.

Chester M, Riley RK, Soltis PS, Soltis DE. 2015. Patterns of chromosomal variation in natural populations of the neoallotetraploid *Tragopogon mirus* (Asteraceae). Heredity **114**, 309–317.

De Smet R, Adams KL, Vandepoele K, Van Montagu MC, Maere S, Van de Peer Y. 2013. Convergent gene loss following gene and genome duplications creates single-copy families in flowering plants. Proceedings of the National Academy of Sciences, USA **110**, 2898–2903.

Dewir YH, Nurmansyah, Naidoo Y, Teixeira da Silva JA. 2018. Thidiazuron-induced abnormalities in plant tissue cultures. Plant Cell Reports **37**, 1451–1470.

Doyle JJ, Doyle JL. 1987. A rapid DNA isolation procedure for small quantities of fresh leaf tissue. Phytochemical Bulletin **19**, 11–15.

Doyle JJ, Coate JE. 2019. Polyploidy, the nucleotype, and novelty: the impact of genome doubling on the biology of the cell. International Journal of Plant Sciences **180**, 1–52.

Evangelisti AM, Conant GC. 2010. Nonrandom survival of gene conversions among yeast ribosomal proteins duplicated through genome doubling. Genome Biology and Evolution **2**, 826–834.

Fox DT, Soltis DE, Soltis PS, Ashman TL, Van de Peer Y. 2020. Polyploidy: a biological force from cells to ecosystems. Trends in Cell Biology **30**, 688–694.

Freeling M. 2009. Bias in plant gene content following different sorts of duplication: tandem, whole-genome, segmental, or by transposition. Annual Review of Plant Biology **60**, 433–453.

Freeling M, Woodhouse MR, Subramaniam S, Turco G, Lisch D, Schnable JC. 2012. Fractionation mutagenesis and similar consequences of mechanisms removing dispensable or less-expressed DNA in plants. Current Opinion in Plant Biology **15**, 131–139.

Gao Q, Luo H, Li Y, Liu Z, Kang C. 2020. Genetic modulation of *RAP* alters fruit coloration in both wild and cultivated strawberry. Plant Biotechnology Journal **18**, 1550–1561.

Ge L, Yong JWH, Goh NK, Chia LS, Tan SN, Ong ES. 2005. Identification of kinetin and kinetin riboside in coconut (*Cocos nucifera* L.) water using a combined approach of liquid chromatography-tandem mass spectrometry,

high performance liquid chromatography and capillary electrophoresis. Journal of Chromatography B **829**, 26–34.

George EF, Hall MA, Klerk GJD. 2008. Plant growth regulators III: gibberellins, ethylene, abscisic acid, their analogues and inhibitors; miscellaneous compounds. In: George EF, Hall MA, Klerk GJD, eds. Plant propagation by tissue culture. Dordrecht: Springer, 227–281.

Gertsson UE. 1988. Influence of macronutrient composition, TIBA and dark treatment on shoot formation and nitrogen content in petiole explants of *Senecio* × *hybridus*. Journal of Horticultural Science **63**, 497–502.

González MN, Massa GA, Andersson M, Turesson H, Olsson N, Fält AS, Storani L, Décima Oneto CA, Hofvander P, Feingold SE. 2020. Reduced enzymatic browning in potato tubers by specific editing of a polyphenol oxidase gene via ribonucleoprotein complexes delivery of the CRISPR/Cas9 system. Frontiers in Plant Science **10**, 1649.

Hanh TT, Lie-Schricke H, Tran Thanh Van K. 1981. Direct *in vitro* bud formation from fragments and thin cell layers of different organs of the winged bean (*Psophocarpus tetragonolobus* L. DC). Journal of Plant Physiology **102**, 127–139.

Helariutta Y, Kotilainen M, Elomaa P, Teeri TH. 1995. *Gerbera hybrida* (Asteraceae) imposes regulation at several anatomical levels during inflorescence development on the gene for dihydroflavonol-4-reductase. Plant Molecular Biology **28**, 935–941.

Hunter DC, Burritt DJ. 2004. Light quality influences adventitious shoot production from cotyledon explants of lettuce (*Lactuca sativa* L.). In Vitro Cellular & Developmental Biology – Plant **40**, 215–220.

Husain MK, Anis M, Shahzad A. 2008. *In vitro* propagation of a multipurpose leguminous tree (*Pterocarpus marsupium* Roxb.) using nodal explants. Acta Physiologiae Plantarum **30**, 353–359.

Ikeuchi M, Ogawa Y, Iwase A, Sugimoto K. 2016. Plant regeneration: cellular origins and molecular mechanisms. Development **143**, 1442–1451.

Ivanova M, Van Staden J. 2009. Nitrogen source, concentration, and NH_4^+:NO_3^- ratio influence shoot regeneration and hyperhydricity in tissue cultured *Aloe polyphylla*. Plant Cell, Tissue and Organ Culture **99**, 167–174.

Jahan AA, Anis M, Aref IM. 2011. Preconditioning of axillary buds in thidiazuron-supplemented liquid media improves *in vitro* shoot multiplication in *Nyctanthes arbor-tristis* L. Applied Biochemistry and Biotechnology **163**, 851–859.

James DJ, Wakerell IJ. 1982. The control of rhizogenesis *in vitro* in difficult-to-root apple rootstocks. In: Fujiwara A, ed. Plant tissue culture. Proceedings of the 5th International Congress of Plant Tissue and Cell Culture. Tokyo and Lake Yamanaka, Japan, July 11–16, 1982. Tokyo, Japan: Japanese Association for Plant Tissue Culture, 187–188.

Jiao Y, Wickett NJ, Ayyampalayam S, ***et al.*** 2011. Ancestral polyploidy in seed plants and angiosperms. Nature **473**, 97–100.

Judd WS, Campbell CS, Kellogg EA, Stevens PF, Donoghue MJ. 2016. Plant systematics: a phylogenetic approach, 4th ed. Sunderland, MA, USA: Sinauer Associates.

Jung YJ, Lee HJ, Kim JH, Kim DH, Kim HK, Cho YG, Bae S, Kang KK. 2019. CRISPR/Cas9-targeted mutagenesis of *F3′ H*, *DFR* and *LDOX*, genes related to anthocyanin biosynthesis in black rice (*Oryza sativa* L.). Plant Biotechnology Reports **13**, 521–531.

Khan MH, Hu L, Zhu M, Zhai Y, Khan SU, Ahmar S, Amoo O, Zhang K, Fan C, Zhou Y. 2021. Targeted mutagenesis of *EOD3* gene in *Brassica napus* L. regulates seed production. Journal of Cellular Physiology **236**, 1996–2007.

Knittel N, Escandón AS, Hahne G. 1991. Plant regeneration at high frequency from mature sunflower cotyledons. Plant Science **73**, 219–226.

Komura S, Kishi-Kaboshi M, Abe F, Inoue Y, Yoshida K. 2025. Improvement of simultaneous genome editing of homoeologous loci in polyploid wheat using CRISPR/Cas9 applying tRNA processing system. Plant Biotechnology **42**, 167–172.

Lander ES. 2016. The heroes of CRISPR. Cell **164**, 18–28.

Landis JB, Soltis DE, Li Z, Marx HE, Barker MS, Tank DC, Soltis PS. 2018. Impact of whole-genome duplication events on diversification rates in angiosperms. American Journal of Botany **105**, 348–363.

Li W, Zhang Y, Liu H, Wang Q, Feng X, Wang C, Sun Y, Zhang X, Zhu S. 2023. Genome-wide identification of putative dihydroflavonol 4-reductase (*DFR*) gene family in eight Solanaceae species and expression analysis in *Solanum lycopersicum*. PeerJ **11**, e16124.

Li Z, Defoort J, Tasdighian S, Maere S, Van de Peer Y, De Smet R. 2016. Gene duplicability of core genes is highly consistent across all angiosperms. The Plant Cell **28**, 326–344.

Lim KY, Soltis DE, Soltis PS, Tate J, Matyasek R, Srubarova H, Kovarik A, Pires JC, Xiong Z, Leitch AR. 2008. Rapid chromosome evolution in recently formed polyploids in *Tragopogon* (Asteraceae). PLoS One **3**, e3353.

Liu X, Feng CM, Franks R, Qu R, Xie DY, Xiang QYJ. 2013. Plant regeneration and genetic transformation of *C. canadensis*: a non-model plant appropriate for investigation of flower development in *Cornus* (Cornaceae). Plant Cell Reports **32**, 77–87.

Lloyd G, McCown B. 1980. Commercially-feasible micropropagation of mountain laurel, Kalmia latifolia, by use of shoot-tip culture. Combined Proceedings, International Plant Propagators' Society **30**, 421–427.

Long Y, Yang Y, Pan G, Shen Y. 2022. New insights into tissue culture plant-regeneration mechanisms. Frontiers in Plant Science **13**, 926752.

Lu CY, Harry IS, Thompson MR, Thorpe TA. 1991. Plantlet regeneration from cultured embryos and seedling parts of red spruce (*Picea rubens* Sarg.). Botanical Gazette **152**, 42–50.

May D, Paldi K, Altpeter F. 2023. Targeted mutagenesis with sequence-specific nucleases for accelerated improvement of polyploid crops: progress, challenges, and prospects. The Plant Genome **16**, e20298.

Mechanda SM, Baum BR, Johnson DA, Arnason JT. 2003. Direct shoot regeneration from leaf segments of mature plants of *Echinacea purpurea* (L.) Moench. In Vitro Cellular & Developmental Biology – Plant **39**, 505–509.

Mohebodini M, Mokhtar JJ, Mahboudi F, Alizadeh H. 2011. Effects of genotype, explant age and growth regulators on callus induction and direct shoot regeneration of Lettuce (*Lactuca sativa* L.). Australian Journal of Crop Science **5**, 92–95.

Mohebodini M, Jalali-Javaran M, Alizadeh H, Mahboudi F, Yarbakht M. 2014. *Agrobacterium*-mediated transformation of lettuce (*Lactuca sativa* L.) to express IgG-binding protein A and human pro-insulin as a fusion protein. The Journal of Horticultural Science and Biotechnology **89**, 719–725.

Murashige T, Skoog F. 1962. A revised medium for rapid growth and bioassays with tobacco tissue cultures. Physiologia Plantarum **15**, 473–497.

Nauerby B, Billing K, Wyndaele R. 1997. Influence of the antibiotic timentin on plant regeneration compared to carbenicillin and cefotaxime in concentrations suitable for elimination of *Agrobacterium tumefaciens*. Plant Science **123**, 169–177.

Ownbey M. 1950. Natural hybridization and amphiploidy in the genus *Tragopogon*. American Journal of Botany **37**, 487–499.

Papp B, Pál C, Hurst LD. 2003. Dosage sensitivity and the evolution of gene families in yeast. Nature **424**, 194–197.

Paterson AH, Chapman BA, Kissinger JC, Bowers JE, Feltus FA, Estill JC. 2006. Many gene and domain families have convergent fates following independent whole-genome duplication events in *Arabidopsis*, *Oryza*, *Saccharomyces* and *Tetraodon*. Trends in Genetics **22**, 597–602.

Phillips GC, Garda M. 2019. Plant tissue culture media and practices: an overview. In Vitro Cellular & Developmental Biology – Plant **55**, 242–257.

Polivanova OB, Bedarev VA. 2022. Hyperhydricity in plant tissue culture. Plants **11**, 3313.

Ramage CM, Williams RR. 2002. Mineral nutrition and plant morphogenesis. In Vitro Cellular & Developmental Biology – Plant **38**, 116–124.

Renny-Byfield S, Wendel JF. 2014. Doubling down on genomes: polyploidy and crop plants. American Journal of Botany **101**, 1711–1725.

Sabbadini S, Capriotti L, Molesini B, Pandolfini T, Navacchi O, Limera C, Ricci A, Mezzetti B. 2019. Comparison of regeneration capacity and *Agrobacterium*-mediated cell transformation efficiency of different cultivars and rootstocks of *Vitis* spp. via organogenesis. Scientific Reports **9**, 582.

Sattler MC, Carvalho CR, Clarindo WR. 2016. The polyploidy and its key role in plant breeding. Planta **243**, 281–296.

Shan S, Boatwright JL, Liu X, Chanderbali AS, Fu C, Soltis PS, Soltis DE. 2020a. Transcriptome dynamics of the inflorescence in reciprocally formed allopolyploid *Tragopogon miscellus* (Asteraceae). Frontiers in Genetics **11**, 888.

Shan S, Gitzendanner MA, Boatwright JL, Spoelhof JP, Ethridge CL, Ji L, Liu X, Soltis PS, Schmitz RJ, Soltis DE. 2024a. Genome-wide DNA methylation dynamics following recent polyploidy in the allotetraploid *Tragopogon miscellus* (Asteraceae). New Phytologist **242**, 1363–1376.

Shan S, Mavrodiev EV, Li R, Zhang Z, Hauser BA, Soltis PS, Soltis DE, Yang B. 2018. Application of CRISPR/Cas9 to *Tragopogon* (Asteraceae), an evolutionary model for the study of polyploidy. Molecular Ecology Resources **18**, 1427–1443.

Shan S, Pisias M, Zhang Z, *et al.* 2024b. Data from: Development of an efficient CRISPR-mediated genome editing platform in the diploid-polyploid model system Tragopogon (Asteraceae). Dryad Digital Repository. https://doi.org/10.5061/dryad.5x69p8dcs

Shan S, Soltis PS, Soltis DE, Yang B. 2020b. Considerations in adapting CRISPR/Cas9 in nongenetic model plant systems. Applications in Plant Sciences **8**, e11314.

Shan S, Yang B, Hauser BA, Soltis PS, Soltis DE. 2023. Developing a CRISPR system in nongenetic model polyploids. In: Van de Peer Y, ed. Polyploidy: methods and protocols. New York: Humana, 475–490.

Shi T, Huang H, Barker MS. 2010. Ancient genome duplications during the evolution of kiwifruit (*Actinidia*) and related Ericales. Annals of Botany **106**, 497–504.

Soltis DE, Buggs RJA, Barbazuk WB, Chamala S, Chester M, Gallagher JP, Schnable PS, Soltis PS. 2012. The early stages of polyploidy: rapid and repeated evolution in *Tragopogon*. In: Soltis PS, Soltis DE, eds. Polyploidy and genome evolution. Berlin, Heidelberg: Springer, 271–292.

Soltis DE, Soltis PS, Pires JC, Kovarik A, Tate JA, Mavrodiev E. 2004. Recent and recurrent polyploidy in *Tragopogon* (Asteraceae): cytogenetic, genomic and genetic comparisons. Biological Journal of the Linnean Society **82**, 485–501.

Soltis PS, Marchant DB, Van de Peer Y, Soltis DE. 2015. Polyploidy and genome evolution in plants. Current Opinion in Genetics & Development **35**, 119–125.

Soltis PS, Soltis DE. 2016. Ancient WGD events as drivers of key innovations in angiosperms. Current Opinion in Plant Biology **30**, 159–165.

Spoelhof JP, Chester M, Rodriguez R, Geraci B, Heo K, Mavrodiev E, Soltis PS, Soltis DE. 2017. Karyotypic variation and pollen stainability in resynthesized allopolyploids *Tragopogon miscellus* and *T. mirus*. American Journal of Botany **104**, 1484–1492.

Symonds VV, Soltis PS, Soltis DE. 2010. Dynamics of polyploid formation in *Tragopogon* (Asteraceae): recurrent formation, gene flow, and population structure. Evolution **64**, 1984–2003.

Tanaka Y, Sasaki N, Ohmiya A. 2008. Biosynthesis of plant pigments: anthocyanins, betalains and carotenoids. The Plant Journal **54**, 733–749.

Tang H, Woodhouse MR, Cheng F, Schnable JC, Pedersen BS, Conant G, Wang X, Freeling M, Pires JC. 2012. Altered patterns of fractionation and exon deletions in *Brassica rapa* support a two-step model of paleohexaploidy. Genetics **190**, 1563–1574.

Tate JA, Joshi P, Soltis KA, Soltis PS, Soltis DE. 2009. On the road to diploidization? Homoeolog loss in independently formed populations of the allopolyploid *Tragopogon miscellus* (Asteraceae). BMC Plant Biology **9**, 80.

Trigiano RN, Vito LM, Windham MT, Boggess S, Hadziabdic D. 2011. Direct shoot organogenesis from leaf explants of Chrysanthemum and African violets. In: Trigiano RN, Gray DJ, eds. Plant tissue culture, development, and biotechnology. Boca Raton, FL, USA: CRC Press, 279–291.

Tripathi JN, Ntui VO, Ron M, Muiruri SK, Britt A, Tripathi L. 2019. CRISPR/Cas9 editing of endogenous *banana streak virus* in the B genome of *Musa* spp. overcomes a major challenge in banana breeding. Communications Biology **2**, 46.

Udall JA, Wendel JF. 2006. Polyploidy and crop improvement. Crop Science **46**, 3–14.

Van de Peer Y, Ashman TL, Soltis PS, Soltis DE. 2021. Polyploidy: an evolutionary and ecological force in stressful times. The Plant Cell **33**, 11–26.

Van Staden J, Drewes SE. 1975. Identification of zeatin and zeatinriboside in coconut milk. Physiologia Plantarum **34**, 106–109.

Wang B, Peng DX, Liu LJ, Sun Z, Zhang N, Gao SM. 2007. An efficient adventitious shoot regeneration system for ramie (*Boehmeria nivea* Gaud) using thidiazuron. Botanical Studies **48**, 173–180.

Wang Y, Tiwari VK, Rawat N, Gill BS, Huo N, You FM, Coleman-Derr D, Gu YQ. 2016. GSP: a web-based platform for designing genome-specific primers in polyploids. Bioinformatics **32**, 2382–2383.

Watanabe K, Kobayashi A, Endo M, Sage-Ono K, Toki S, Ono M. 2017. CRISPR/Cas9-mediated mutagenesis of the *dihydroflavonol-4-reductase-B* (*DFR-B*) locus in the Japanese morning glory *Ipomoea* (*Pharbitis*) *nil*. Scientific Reports **7**, 10028.

Wendel JF, Flagel LE, Adams KL. 2012. Jeans, genes, and genomes: cotton as a model for studying polyploidy. In: Soltis PS, Soltis DE, eds. Polyploidy and genome evolution. Berlin, Heidelberg: Springer, 181–207.

Wendel JF. 2015. The wondrous cycles of polyploidy in plants. American Journal of Botany **102**, 1753–1756.

Wendel JF, Lisch D, Hu G, Mason AS. 2018. The long and short of doubling down: polyploidy, epigenetics, and the temporal dynamics of genome fractionation. Current Opinion in Genetics & Development **49**, 1–7.

Wood TE, Takebayashi N, Barker MS, Mayrose I, Greenspoon PB, Rieseberg LH. 2009. The frequency of polyploid speciation in vascular plants. Proceedings of the National Academy of Sciences, USA **106**, 13875–13879.

Ye S, Cai C, Ren H, Wang W, Xiang M, Tang X, Zhu C, Yin T, Zhang L, Zhu Q. 2017. An efficient plant regeneration and transformation system of ma bamboo (*Dendrocalamus latiflorus* Munro) started from young shoot as explant. Frontiers in Plant Science **8**, 1298.

Yong JWH, Ge L, Ng YF, Tan SN. 2009. The chemical composition and biological properties of coconut (*Cocos nucifera* L.) water. Molecules **14**, 5144–5164.

Yoo MJ, Koh J, Boatwright JL, Soltis DE, Soltis PS, Barbazuk WB, Chen S. 2024. Investigation of regulatory divergence between homoeologs in the recently formed allopolyploids, *Tragopogon mirus* and *T. miscellus* (Asteraceae). The Plant Journal **117**, 1191–1205.

Zaytseva YG, Skaptsov MV, Kutsev MG, Novikova NT. 2020. *In vitro* establishment and TDZ-induced regeneration from shoot and leaf explants of *Rhododendron sichotense* Pojark. Turczaninowia **23**, 106–111.

Ziemienowicz A. 2014. *Agrobacterium*-mediated plant transformation: factors, applications and recent advances. Biocatalysis and Agricultural Biotechnology **3**, 95–102.